Wrinkled Rh_2P Nanosheets as Superior pH-universal Electrocatalysts for Hydrogen Evolution Catalysis

*Kai Wang[&], Bolong Huang[&], Fei Lin, Fan Lv, Minchuan Luo, Peng Zhou, Qiao Liu, Weiyu Zhang, Chao Yang, Yonghua Tang, Yong Yang, Wei Wang, Hao Wang and Shaojun Guo**

Mr. K. Wang, Mr. F. Lin，Mr. F. Lv, Dr. M. Luo, Dr. P. Zhou, Ms. W. Zhang, Mr. C. Yang, Mr. Y. Tang, Dr. Y. Yang, Dr. W. Wang and Prof. S. Guo
Department of Materials Science and Engineering, College of Engineering, Peking University, Beijing 100871, China
E-mail: guosj@pku.edu.cn

Dr. B. Huang
Department of Applied Biology and Chemical Technology, The Hong Kong Polytechnic University, Hung Hom, Kowloon, Hong Kong SAR, China.

Mr. Q. Liu and Prof. H. Wang
Laboratory of Heat and Mass Transport at Micro-Nano Scale, College of Engineering, Peking University, Beijing 100871, China.

Prof. S. Guo
BIC-ESAT, College of Engineering, Peking University, Beijing 100871, China.

[&] Equal Contribution

Keywords: heterogeneous catalysts, metal phosphides, wrinkled structure, two-dimensional, hydrogen evolution reaction

Abstract

Searching the highly efficient and durable electrocatalysts toward hydrogen evolution reaction (HER) at all pH is of great interest to the scientific community, however is still a grand challenge because the HER kinetics of Pt in alkaline solutions is approximately two to three orders of magnitude lower than that in acidic solution. Herein, we report a new class of wrinkled, ultrathin Rh_2P nanosheets for enhancing HER catalysis at all pH. They exhibit a small overpotential of 18.3 mV at 10 mA cm^{-2}, low Tafel slope of 61.5 mV dec^{-1} and good durability in alkaline media, much better than the commercial Pt/C catalyst. Density functional theory (DFT) calculations reveal that the active open-shell effect from P-3p band not only promotes Rh-4d for higher activities of

proton-electron charge exchange but also provides stronger capabilities of excellent p-p overlapping to locate the O-related species as distributary center, which can benefit the HER process in alkaline media. We also demonstrate that the present wrinkled, ultrathin Rh_2P nanosheets are highly efficient and durable electrocatalysts toward HER in both acid and neutral electrolytes. The present work opens a new material design for ultrathin 2D metal phosphides nanostructures in boosting HER at all pH.

Hydrogen (H_2) has been considered a green and renewable resource alternative to reduce our dependence on fossil fuels to benefit the environment.[1] The hydrogen evolution reaction (HER) is a crucial step in electrochemical water splitting, and plays an important role in energy conversion for the development of hydrogen-based energy resources.[2] For an energy-efficient HER, a catalyst must be able to trigger the proton reduction with minimal overpotential and fast kinetics.[3] Recently, the pH-universal nanoelectrocatalysts for HER have drawn a lot of attention as they could work well with the good oxygen evolution reaction (OER) catalysts in the same electrolyte regardless of pH.[4] Platinum (Pt) is generally considered as the best state-of-the-art catalysts towards HER, particularly in acid media due to its highest exchange current density and lowest Tafel slope.[5] However, the HER kinetics of Pt in alkaline solutions is usually approximately two to three orders of magnitude lower than that in acidic solutions, hindering its practical use in electrochemical water splitting.[3] Besides, in industrial manufacture, acid electrolytic cell, normally operating at high temperatures, inevitably produces the electrolyte vapor or acid fog that can contaminate the hydrogen gas but also corrode the used devices, while alkaline electrolyzer generally works in a lower vapor pressure under

the higher temperature conditions and can generate high purity hydrogen.[6] As a consequence, it is very urgent to develop an effective and highly efficient HER nanoelectrocatalyst that can work very well at all pH, especially in the alkaline media.[7] To date, metal phosphides,[8] carbides,[9] sulphides[10] and heteroatom-doped (*e.g.* N, P, S) carbon nanomaterials[11] have been proved to be good nanoelctrocatalysts toward HER under various pH values as they could tune the water dissociation free energy and hydrogen adsorption free energy well for HER.[12] However, the reported nanoelectrocatalysts can merely exhibit Pt-like HER activity. It remains a grand challenge to search for a Pt-free electrocatalyst that can boost HER at all pH and exhibit better HER activity than that of commercial Pt/C.[13]

Herein, we design novel wrinkled, ultrathin Rh_2P nanosheets as a highly efficient pH-universal electrocatalyst for HER, which is superior to commercial Pt/C, especially in alkaline media. They exhibit a smaller overpotential of 18.3 mV at 10 mA cm^{-2}, lower Tafel slopes of 61.5 mV dec^{-1} and better durability (negligible activity decay after 1000 potential sweeps) than those of commercial Pt/C in alkaline media. Density functional theory (DFT) calculations were used to shed the light on the catalytic mechanism in alkaline solution, which indicates that the activities of d-bands in transition metals (Rh-4d) can be boosted up by open-shell P-3p orbital for both effective charge-transfer and binding of the O-related species. This would provide a key reason of high HER performance by a series of transition metal phosphides, especially in alkaline media. Besides, the wrinkled Rh_2P nanosheets were also demonstrated to work very well as highly efficient and durable electrocatalysts toward HER in both acid and neutral electrolytes.

Wrinkled Rh_2P nanosheets were prepared *via* a two-step chemical procedure. Rh nanosheets were firstly synthesized by using $Rh(acac)_3$ and $Ni(acac)_2$ as metal precursors, ascorbic acid (AA) as reductant, oleylamine (OAm) as solvent and surfactant and carbon monoxide decomposed by $Mo(CO)_6$ at 180 °C as a surface confining agent. Then, they were phosphorized at high temperature of 300 °C with phosphorus through the decomposition of tri-n-octylphosphine (TOP) under air free condition.[14] The wrinkled Rh_2P nanosheets preserve the ultrathin 2D structure of Rh nanosheets after high temperature phosphorization process.

Transmission electron microscopy (TEM), high-angle annular dark-field scanning TEM (HAADF-STEM), power X-ray diffraction (PXRD), high-resolution transmission electron microscopy (HRTEM) and selected-area electron diffraction (SAED) were used to characterize ultrathin Rh nanosheets and wrinkled Rh_2P nanosheets. **Figure 1a&1b** show that the as-made Rh nanosheets with high yield have an average diameter of *ca.* 250 nm. PXRD of Rh nanosheets (**Figure S1a**) shows a few of diffraction peaks, assigned to the (100), (200) and (220) reflections of cubic (*Fm-3m*) Rh [Joint Committee on Powder Diffraction Standards (JCPDS) No. 05-0685].[15] The TEM energy-dispersive X-ray spectroscopy (TEM-EDX) spectra (**Figure S1b**) were further employed to characterize the chemical composition of the Rh nanosheets. No Ni and Mo atoms can be detected, indicating the formation of pure Rh nanosheets. HRTEM (**Figure 1c**) and SAED image of one single nanoplate prove the low crystallinity of the Rh nanosheets (**Figure S1c&S1d**), being in accordance with the PXRD result. Herein, we found that the existence of $Ni(acac)_2$ and AA was necessary for the synthesis of high-quality Rh nanosheets (**Figure S2&S3**). And also carbon monoxide decomposed by $Mo(CO)_6$ as a surface confining agent was the key in formation of Rh

nanosheets since only nanoparticles could be obtained without the existence of $Mo(CO)_6$ (**Figure S4**).

The Rh nanosheets were then phosphorized with phosphorus by the decomposition of Tri-n-octylphosphine (TOP) under air free conditions (details in Experimental Section) to make the wrinkled Rh_2P nanosheets. **Figure 1d&S5** show the representative HAADF-STEM and TEM images of the wrinkled Rh_2P nanosheets. They preserve the ultrathin 2D morphology of Rh nanosheets after high-temperature phosphorization process. The thickness of wrinkled Rh_2P nanosheets was determined to be about 3.3 nm (**Figure S6**) by atomic force microscopy (AFM), proving their ultrathin feature. **Figure 1e** shows the representative TEM image and the related SAED image (*inset*) of one single wrinkled Rh_2P nanosheet, showing its polycrystalline structure. The HRTEM image of the wrinkled Rh_2P nanosheets is displayed in **Figure 1f**, in which the lattice spacings of 0.276 nm and 0.196 nm correspond to the (200) and (220) planes, respectively. The elemental distribution of Rh and P of the wrinkled Rh_2P nanosheets was characterized using STEM-energy dispersive X-ray spectroscopy (EDX) mapping (**Figure 1g**), where Rh and P elements distribute uniformly across the whole nanosheet, and the compositional ratio of Rh to P in wrinkled Rh_2P nanosheets is determined to be *ca.* 2:1 by EDX analysis (**Figure 1h**), being in accordance with the results of inductively coupled plasma atomic emission spectroscopy (ICP-AES) and X-ray photoelectron spectroscopy (XPS). PXRD pattern of the wrinkled Rh_2P nanosheets shows that they are highly crystalline with cubic (*Fm-3m*) Rh_2P structure (**Figure 1i**, JCPDS No. 02-1299).[16] X-ray photoelectron spectroscopy (XPS) was also used to study the chemical states of Rh and P after the phosphorization process (**Figure 1j**). All the binding energies were calibrated to C 1s carbon at 284.8 eV to eliminate

differences in sample charging. For the wrinkled Rh_2P nanosheets (**Figure 1j&S7**), the XPS spectrum in the Rh 3d 5/2 region shows the peaks at 307.8 eV and 321.5 eV (with well separated spin-orbit components, Δ_{metal} = 4.7 eV), which are slightly above the binding energy for Rh metal (307.0-307.6 eV) and well below the value for Rh^{3+} in Rh_2O_3 (308.8 eV), indicating that Rh in wrinkled Rh_2P nanosheets bears a partial positive charge ($Rh^{\delta+}$),[17] quite different from Rh atoms in Rh nanosheets existing mainly in oxidized state (Rh^{3+}) due to surface oxidation (**Figure S8**). The broad P 2p XPS peak is fitted into three peaks. The peaks located at 130.3 and 131.2 eV are attributed to the P 2p 3/2 orbitals of metal phosphide while the peak centered at 133.5 eV is attributed to P 2p 1/2 orbitals of residual metal phosphates due to surface partially oxidation,[18] proving the phosphorized Rh nanosheets exist mainly in the state of Rh_2P.

The HER catalytic activity of wrinkled Rh_2P nanosheets and Rh nanosheets were evaluated by recording polarization curves in N_2-saturated 0.1 M KOH (with IR corrected) with a scan rate of 5 mV s^{-1} at room temperature. The commercial Pt/C (20 wt %) was also studied as the benchmark catalyst under the same conditions. Before the electrochemical measurement, the wrinkled Rh_2P nanosheets and Rh nanosheets were deposited on a commercial carbon (Ketjen-300J) support (**Figure S9&S10**, named as w-Rh_2P NS/C and Rh NS/C, respectively). The carbon supported w-Rh_2P NS/C and Rh NS/C, dispersed in a mixture of isopropanol/water/Nafion solution, were casted onto a rotating disk electrode. **Figure 2a** shows that among all the investigated samples, w-Rh_2P NS/C displays the best HER catalytic activity in 0.1 M KOH solution. It exhibits an overpotential (η) of 18.3 mV at a current density of 10 mA cm^{-2}, (**Figure 2b**), 40.1 mV lower than that of commercial Pt/C (58.4 mV) and 50.6 mV lower than that of Rh NS/C (68.9 mV), indicating

the superior catalytic activity of w-Rh_2P NS/C in alkaline media. The Tafel slopes were obtained according to the Tafel equation: ($\eta = b \times \log(j) + a$, where b is the Tafel slope) in a linear region of the Tafel plots.[19] As shown in **Figure 2c**, the Tafel slopes are 61.5, 87.4 and 113 mV dec^{-1} for w-Rh_2P NS/C, Pt/C and Rh NS/C, respectively, suggesting that the w-Rh_2P NS/C exhibits more favorable kinetics toward HER catalysis than the Pt/C and w-Rh NS/C. Note that both the overpotential and Tafel slope of w-Rh_2P NS /C are lower than those of Pt/C, Rh NS/C and most of the reported state-of-the-art electocatalysts in alkaline media (**Table S1**), further indicating the superior electrocatalytic activity of w-Rh_2P NS/C.

Besides, the electrochemical stability of w-Rh_2P NS /C, Pt/C and Rh NS/C was also evaluated using a long-term cycling test in 0.1 M KOH. As shown in **Figure 2d**, the polarization curve of w-Rh_2P NS/C shows negligible negative shift after 1000 cyclic voltammetry (CV) cycles. As for Pt/C and Rh NS/C, their polarization curves show obvious negative shift under the same condition (**Figure S11**), indicating a significant decrease in the electrocatalytic activities of Pt/C and Rh NS/C. The above results indicate that the ultrathin 2D wrinkled Rh_2P nanosheets are highly efficient and durable electrocatalysts toward HER in alkaline media.

To shed the lights on the catalytic mechanism in alkaline solution, an in-depth investigation of the entire hydrogen evolution reaction on both Rh_2P NS and Rh NS was carried out. The Rh_2P (*Fm-3m*) surface (200) model has been built. The final structure shows a substantial reconstruction and lowers the system energy with the magnitude of -3.21 $eV \cdot nm^{-2}$. The charge density distribution of bonding and antibonding orbitals has turned from nearly-delocalized to localized by following the reconstruction (**Figure 3a**). To exhibit the subtle information on the Rh-P bonding, we performed the

previously developed *ab-initio* method on projecting the on-site orbital potential components with orbital electronic chemical potential and screened pseudo charge compensated orbital relaxation. This reflects the electronic activities of the targeted orbital especially with electronic occupation within different chemical bonding environment. It is found that the Rh-4d orbital turns to be a closed shell (crossover), indicating strong orbital overlaps between Rh and neighboring P sites. While the P-3p orbital gets to active open-shell effect (non-crossover), providing more abundant accommodations for charge exchange (**Figure S12**). The shown closed shell effect for Rh site repulsively promotes the 4d-electrons to occupy the higher energies with 4d-band closer to the Fermi level (E_F), compared to the Rh_2P (111), Rh_2P bulk, and Rh-metal (**Figure 3b**). To dates, the band width, band shapes, band centers, and band overlapping have been being still actively discussed to emphasize many contributing roles of catalyst, including the stabilities, catalytic activities, *etc*. These can also determine the performance of catalysts.[20] We further found the orbital interplay for Rh and P sites is different from the internal bulk to the surface. In addition, the bonding capability for P-3p to overlap the O-2p would be potentially reduced if the Rh-4d band covers a wide range of P-3p band due to the delocalized behavior on the (111) surface (**Figure 3c**). This effect has been alleviated on the Rh_2P (200) surface. The Rh-4d and P-3p bands have been clearly discrete, and the P-3p orbital shows a strongly localization for potentially bonding of O-2p from the species of H_2O and OH group. This is confirmed by the substantial p-band matching between O-2p from H_2O and P-3p orbitals (**Figure 3d**).

The pathway for HER under alkaline condition has been studied between Rh_2P (200) and Rh (100) surfaces (**Figure 3e**). Overall, the Rh_2P (200) (-2.14 eV) shows more energetic favorable than

that in the Rh (100) (-0.77 eV) for HER. The initial adsorption of itinerant H_2O and [H^++ e^-] is similar to both system with -1.89 eV for Rh_2P (200) and -1.74 eV for Rh (100) respectively. However, due to the strong over-binding effect (Rh-H) on the Rh (100) surface, the location and splitting of the H_2O meets the energetic barriers. Especially to the step of splitting from [H_2O*+*(H^++e^-)] to [*OH^-+2*H^++e^-], which is the potentially the barrier energetic difference of 0.62 eV, implying the endothermic reaction heat for the path. In contrast, the HER on the Rh_2P (200) surface turns to be a barrier free pathway. The further binding energy studies confirm the moderate Rh-H bonding for Rh_2P (200) but much stronger on the Rh (100) surface. It implies a potential further bond cleave of H-H to reverse the 2*H→H_2 backward. The chemisorption energies also exhibit an obvious contrast between these two systems. It is shown that the H and H_2 chemisorption energies in the Rh_2P (200) system are close to the thermoneutral line ($\Delta G = 0$), where denotes an efficient adsorption and desorption. This confirms the processes for both 2*H→2H→H_2 and H_2-desorption are rather energetic favorable. However, the chemisorption energies in the Rh (100) system display much descent energy levels, confirming that the over-binding potentially decreases the efficiency of HER. From the local structure (**Figure S13**), the stable adsorbed H is bonding with Rh site and the sole H_2O location is also staying near the Rh-site. The H_2O molecule is weakly bonded on the top of surface Rh site while the OH group is strongly binding with the surface Rh-site. The H_2O splitting process occurs on the surface Rh sites. The two closely contacted adsorbed *H actually exhibit head-to-head structural configuration for potentially efficient H_2 generation. With the assistance of P site, the leaving group (OH^-) can be stably located on the surface of Rh_2P (200). We have performed the comparison on free energy pathways (ΔG) for HER under alkaline condition,

with consideration of P-terminated (P_T-Rh_2P (200)), Rh-terminated (Rh_T-Rh_2P (200)), and Rh (100) surfaces, respectively (**Figure 3e**). We have found out the potential over-binding issue with hydroxyl groups [*OH-] led by P-terminated surface of Rh_2P (200) under the alkaline solution condition. Especially, this over-binding effect may go further severely when the OH-contained solution adsorption coverage turns to be even higher. Accordingly, the OH species adsorbed on the Rh-site will easily have desorption or detachment, while the P surface sites would unlikely have this since the (P-3p)-(O-2p) overlapping would increase the probabilities of overbinding or surface P-oxidation states. Therefore, the Rh_T-Rh_2P (200) can be long-sustainable for pH-universal HER electrochemical environment. The observed active open-shell effect from P-3p band not only promotes Rh-4d for higher activities of proton-electron charge exchange but also provides stronger capabilities of p-p overlapping to locate the O-related species, which can facilitate the HER process in alkaline media.

The HER performance of w-Rh_2P NS/C, Pt/C and Rh NS/C was investigated in 0.1 M $HClO_4$ as well. As shown in **Figure 4a**, the w-Rh_2P NS/C displays the best HER catalytic activity among all three samples in 0.1 M $HClO_4$. In 0.1 M $HClO_4$, to reach a current density of 10 mA cm^{-2}, the overpotential required for Rh_2P NS /C is only 15.8 mV (**Figure 4b**), 6.3 mV and 25.8 mV lower than those of commercial Pt/C (22.1 mV) and Rh NS/C (41.6 mV). Besides, the Tafel slope is 29.9 mV dec^{-1} for w-Rh_2P NS /C (**Figure 4b&S14**), comparable to that of commercial Pt/C (29.6 mV dec^{-1}) and lower than that of Rh NS/C (37.4 mV dec^{-1}), suggesting it employs the Volmer-Tafel mechanism ($H_{ads} + H_{ads} \rightarrow H_2\uparrow$) for HER.[21] The HER performance of w-Rh_2P NS /C was further studied in 0.5 M PBS solution. Remarkably, the Rh_2P NS /C still displays the best HER catalytic activity in neutral media (**Figure 4c**) with a small overpotential of 21.9 mV to achieve a current density of 10 mA cm^{-2}

(**Figure 4d**), lower than those of Pt/C (27.2 mV) and Rh NS/C (47.7 mV). Meanwhile, w-Rh_2P NS/C shows a Tafel slope of 78.4 mV dec^{-1}, comparable to that of Pt/C. Besides, the w-Rh_2P NS/C displays better stabilbity than that of Pt/C and Rh NS/C in 0.1 M $HClO_4$ and 0.5 M PBS. (**Figure S15&S16**) These results prove that the wrinkled Rh_2P nanosheets could serve as the superior Pt-free pH-universal electrocatalysts for HER.

Conclusions

In summary, we have successfully designed a new class of wrinkled Rh_2P nanosheets for boosting HER at all pH. Particularly, in 0.1 M KOH solution, the wrinkled Rh_2P nanosheets are more efficient and durable for HER by showing smaller overpotential, lower Tafel slope and much lower activity decay after long-time cycles than those of commercial Pt/C. DFT calculations interpret the P-3p orbital with open-shell behavior reserves an optimal role in leveling-up the Rh-4d band for highly active charge exchange with protons *via* orbital Coulombic interactions. Moreover, the lower-lying 3p-σ bonding level guarantees the effectiveness of locating O-related species as perfect distributary center, which can further benefit the HER performance in alkaline media. The present wrinkled, ultrathin Rh_2P nanosheets are also highly general for catalyzing HER in both acid and neutral electrolytes, which are superior to commercial Pt/C catalyst. This work first highlights the important role of designing ultrathin metal phosphide nanosheets as pH-universal electrocatalysts for HER with both excellent electrocatalytic activity and stability.

Supporting Information

Supporting Information is available from the Wiley Online Library or from the author.

Acknowledgements

This work was financially supported by the National Natural Science Foundation of China (51671003), the National Key Research and Development Program of China (No. 2017YFA0206701), the Open Project Foundation of State Key Laboratory of Chemical Resource Engineering, and the start-up support from Peking University and the Young Thousand Talented Program.

Received: ((will be filled in by the editorial staff))
Revised: ((will be filled in by the editorial staff))
Published online: ((will be filled in by the editorial staff))

References

[1] a) G. W. Crabtree, M. S. Dresselhaus, M. V. Buchanan, *Phys. Today* **2004**, 57, 39; b) M. G. Walter, E. L. Warren, J. R. McKone, S. W. Boettcher, Q. Mi, E. A. Santori, N. S. Lewis, *Chem. Rev.* **2010**, 110, 6446; c) M. Dresselhaus, I. Thomas, *Nature* **2001**, 414, 332.

[2] a) Y. Zheng, Y. Jiao, M. Jaroniec, S. Z. Qiao, *Angew. Chem. Int. Ed.* **2015**, 54, 52; b) Y. Shi, B. Zhang, *Chem. Rev.* **2016**, 45, 1529; c) S. Dou, L. Tao, R. Wang, S. El Hankari, R. Chen, S. Wang, *Adv. Mater.* **2018,** 30, 1705850; d) Z. Xiao, Y. Wang, Y.-C. Huang, Z. Wei, C.-L. Dong, J. Ma, S. Shen, Y. Li, S. Wang, *Energy Environ. Sci.* **2017,** 10, 2563.

[3] a) Y. Zheng, Y. Jiao, S. Qiao, A. Vasileff, *Angew. Chem. Int. Ed., 10.1002/anie.201710556 (2017)*; b)

[4] a) J. Mahmood, F. Li, S.-M. Jung, M. S. Okyay, I. Ahmad, S.-J. Kim, N. Park, H. Y. Jeong, J.-B. Baek, *Nat. Nanotech.* **2017**, 12, 441; b) J. Yin, Q. Fan, Y. Li, F. Cheng, P. Zhou, P. Xi, S. Sun, *J. Am. Chem. Soc.* **2016**, 138, 14546; c) A. Han, H. Chen, H. Zhang, Z. Sun, P. Du, *J. Mater. Chem. A* **2016**,

4, 10195; d) X. Zou, X. Huang, A. Goswami, R. Silva, B. R. Sathe, E. Mikmeková, T. Asefa, *Angew. Chem. Int. Ed.* **2014**, 126, 4461.

[5] a) J. K. Nørskov, T. Bligaard, A. Logadottir, J. Kitchin, J. G. Chen, S. Pandelov, U. Stimming, *J. Electrochem. Soc.* **2005**, 152, J23; b) J. Greeley, T. F. Jaramillo, J. Bonde, I. Chorkendorff, J. K. Nørskov, *Nat. Mater.* **2006**, 5, 909.

[6] J. Wang, F. Xu, H. Jin, Y. Chen, Y. Wang, *Adv. Mater.* **2017,** 29, 1605838.

[7] a) W. Sheng, M. Myint, J. G. Chen, Y. Yan, *Energy Environ. Sci.* **2013**, 6, 1509; b) W. Sheng, H. A. Gasteiger, Y. Shao-Horn, *J. Electrochem. Soc.* **2010**, 157, B1529.

[8] a) J. F. Callejas, C. G. Read, C. W. Roske, N. S. Lewis, R. E. Schaak, *Chem. Mater.* **2016**, 28, 6017; b) J. Tian, Q. Liu, A. M. Asiri, X. Sun, *J. Am. Chem. Soc.* **2014**, 136, 7587; c) Y. Zeng, Y. Wang, G. Huang, C. Chen, L. Huang, R. Chen, S. Wang, *Chem. Commun.* **2018,** 54, 1465.

[9] a) C. Wan, Y. N. Regmi, B. M. Leonard, *Angew. Chem. Int. Ed.* **2014**, 126, 6525; b) H. Lin, Z. Shi, S. He, X. Yu, S. Wang, Q. Gao, Y. Tang, *Chem. Sci.* **2016**, 7, 3399; c) H. Lin, W. Zhang, Z. Shi, M. Che, X. Yu, Y. Tang, Q. Gao, *ChemSusChem* **2017**, 10, 2597.

[10] a) T. F. Jaramillo, K. P. Jørgensen, J. Bonde, J. H. Nielsen, S. Horch, I. Chorkendorff, *Science* **2007**, 317, 100; b) G. Kalaiyarasan, K. Aswathi, J. Joseph, *Int. J. Hydrogen Energy* **2017**, 42, 22866.

[11] a) X. Zou, Y. Zhang, *Chem. Soc. Rev.* **2015**, 44, 5148; b) H. Tabassum, W. Guo, W. Meng, A. Mahmood, R. Zhao, Q. Wang, R. Zou, *Adv. Energy Mater.* **2017,** 7, *1601671.*

[12] G.-f. Long, K. Wan, M.-y. Liu, Z.-x. Liang, J.-h. Piao, P. Tsiakaras, *J. Catal.* **2017**, 348, 151.

[13] a) M. K. Debe, *Nature* **2012**, 486, 43; b) V. S. Thoi, Y. Sun, J. R. Long, C. J. Chang, *Chem. Soc. Rev.* **2013**, 42, 2388.

[14] A. Mendoza‐Garcia, H. Zhu, Y. Yu, Q. Li, L. Zhou, D. Su, M. J. Kramer, S. Sun, *Angew. Chem. Int. Ed.* **2015**, 54, 9642.

[15] N. Zhang, Q. Shao, Y. Pi, J. Guo, X. Huang, *Chem. Mater.* **2017***,* 28, 6017.

[16] H. Duan, D. Li, Y. Tang, Y. He, S. Ji, R. Wang, H. Lv, P. P. Lopes, A. P. Paulikas, H. Li, *J. Am. Chem. Soc* **2017**, 139, 5494.

[17] J. R. Hayes, R. H. Bowker, A. F. Gaudette, M. C. Smith, C. E. Moak, C. Y. Nam, T. K. Pratum, M. E. Bussell, *J. Catal.* **2010**, 276, 249.

[18] C.-C. Hou, Q. Li, C.-J. Wang, C.-Y. Peng, Q.-Q. Chen, H.-F. Ye, W.-F. Fu, C.-M. Che, N. López, Y. Chen, *Energy Environ. Sci.* **2017**, 10, 1770.

[19] K. Xu, H. Ding, M. Zhang, M. Chen, Z. Hao, L. Zhang, C. Wu, Y. Xie, *Adv. Mater.* **2017**, 29, 1606980.

[20] a) H. Xin, A. Vojvodic, J. Voss, J. K. Nørskov, F. Abild-Pedersen, *Phys. Rev. B* **2014,** 89, 115114; b) N. Acerbi, S. Tsang, G. Jones, S. Golunski, P. Collier, *Angew. Chem. Int. Ed.* **2013,** 52, 7737; c) F. Lima, J. Zhang, M. Shao, K. Sasaki, M. Vukmirovic, E. Ticianelli, R. Adzic, *J. Phys. Chem. C* **2007,** 111, 404.

[21] a) E. Skúlason, V. Tripkovic, M. E. Björketun, S. d. Gudmundsdóttir, G. Karlberg, J. Rossmeisl, T. Bligaard, H. Jónsson, J. K. Nørskov, *J. Phys. Chem. C* **2010**, 114, 18182; b) Z. Pu, I. S. Amiinu, Z. Kou, W. Li, S. Mu, *Angew. Chem. Int. Ed.* **2017,** 56, 11559.

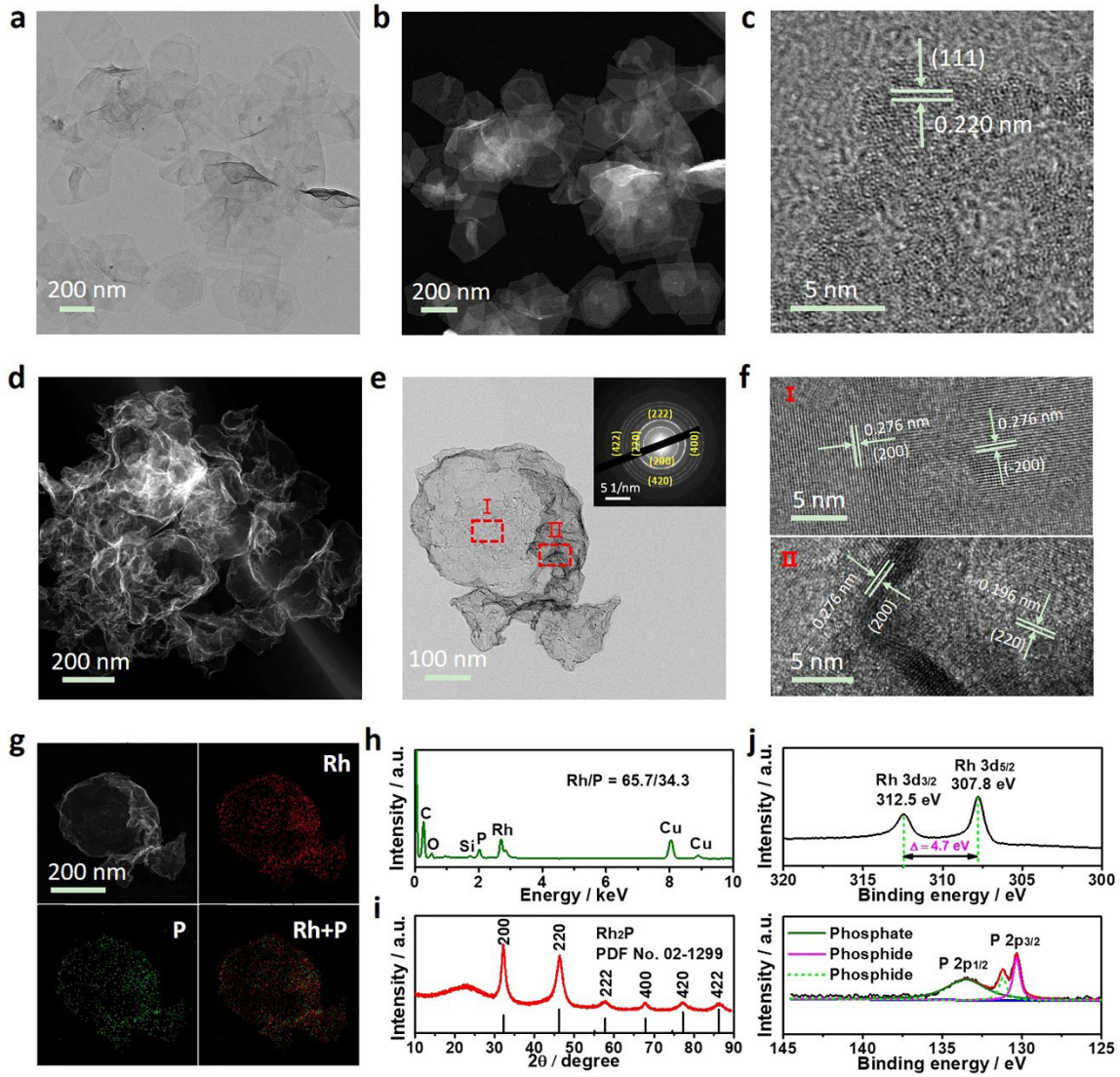

Figure 1. Morphology and structure characterization of Rh nanosheets and wrinkled Rh_2P nanosheets. Representative (a) TEM image and (b) HAADF-STEM image of nanosheets. (c) HRTEM TEM image of Rh nanosheets. (d) Representative HAADF-STEM image of wrinkled Rh_2P nanosheets. (e) TEM image of one single wrinkled Rh_2P nanosheets. The *inset* shows the corresponding SAED image. (f) HRTEM, (g) STEM-EDX elemental mapping, (h) STEM-EDX spectrum and (i) PXRD pattern of wrinkled Rh_2P nanosheets. (j) XPS analysis of Rh 3d and P 2p for wrinkled Rh_2P nanosheets.

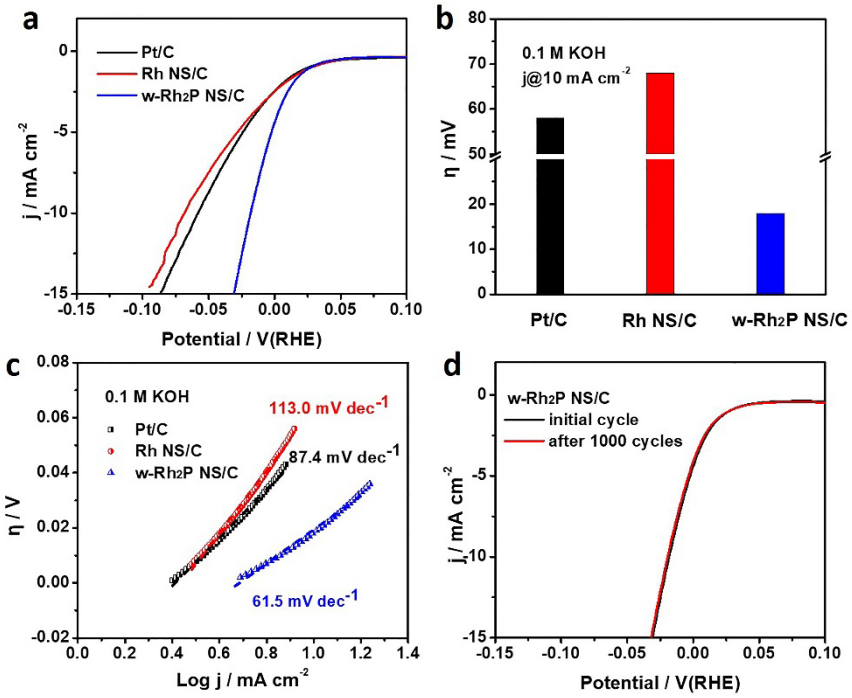

Figure 2. Electrocatalytic activities of Pt/C, Rh NS/C and w-Rh_2P NS/C in 0.1 M KOH. (a) HER polarization curves, (b) overpotentials at 10 mA cm^{-2} and (c) Tafel slopes of different catalysts. (d) Electrochemical stability of w-Rh_2P NS/C.

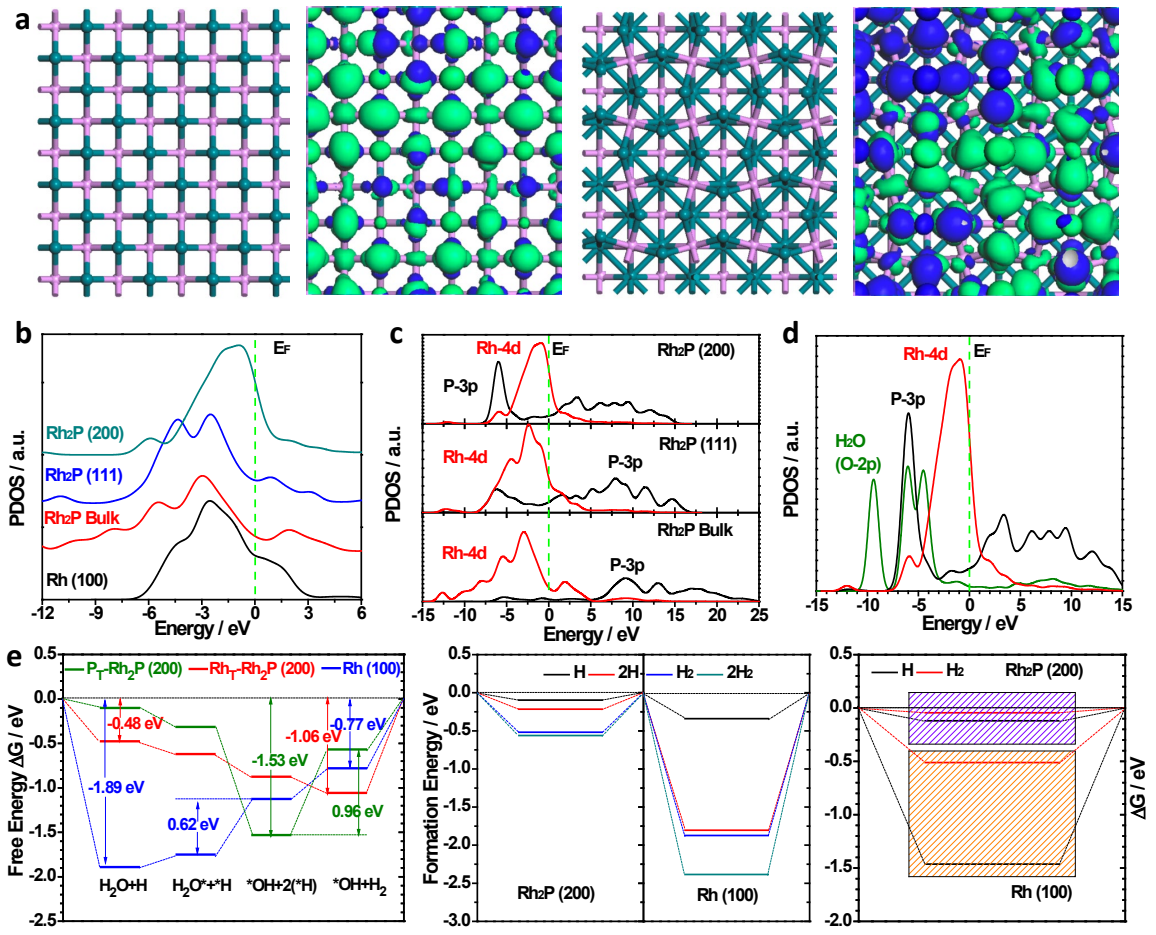

Figure 3. DFT simulations of HER. (a) The Rh_2P (200) surface lattice before and after reconstruction with charge density distributions. (b) The projected density of states (PDOS) for the Rh-4d bands within Rh_2P (200), Rh_2P (111), Rh_2P bulk, and Rh-metal. (c) The PDOS for the Rh-4d and P-3p bands for illustrating the overlapping effect. (d) Overlapping effect among the Rh-4d, P-3p and O-2p from H_2O shown by PDOS. (e) Free energy pathways (ΔG) for HER of P-terminated (P_T-Rh_2P (200)), Rh-terminated (Rh_T-Rh_2P (200)), and Rh (100) surfaces, respectively, under alkaline condition as well as the formation energies of H, 2H, H_2 and $2H_2$ contrasted by the chemisorption energies between Rh_2P (200) and Rh (100) surfaces.

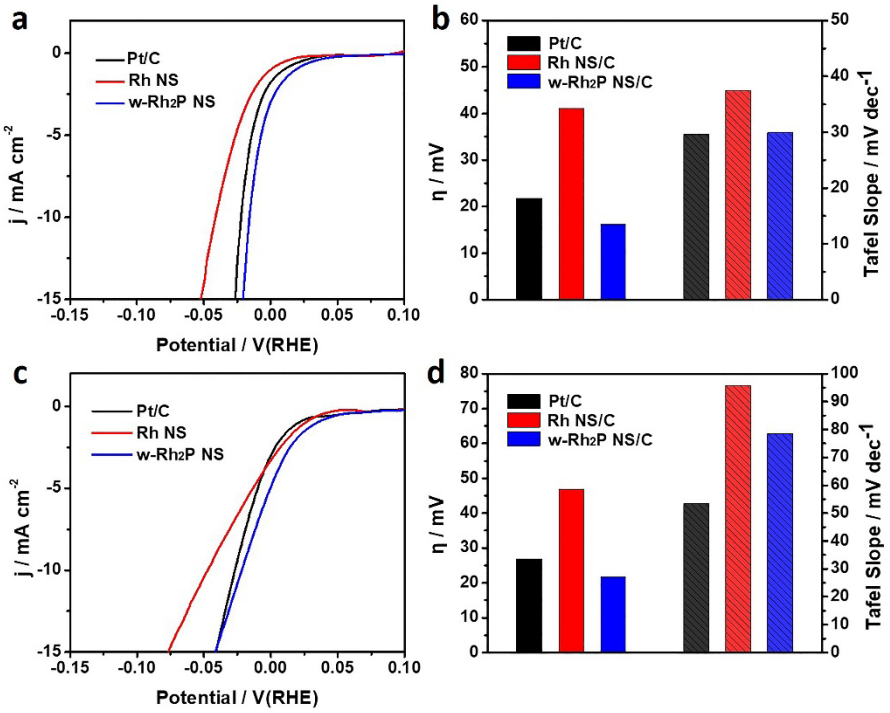

Figure 4. Electrocatalytic activities of Pt/C, Rh NS/C and w-Rh_2P NS/C in 0.1 M $HClO_4$ and 0.5 M PBS. (a) HER polarization curves, (b) overpotentials at 10 mA cm^{-2} and Tafel slopes of Pt/C, Rh NS/C and w-Rh_2P NS/C in 0.1 M $HClO_4$. (c) HER polarization curves and (d) overpotentials at 10 mA cm^{-2} and Tafel slopes of Pt/C, Rh NS/C and w-Rh_2P NS/C in 0.5 M PBS.

The table of contents entry

We report a novel wrinkled ultrathin Rh_2P nanosheets as pH-universal electrocatalysts for HER, which are more efficient and durable than commercial Pt/C, especially in alkaline media. The wrinkled ultrathin Rh_2P nanosheets exhibit a small overpotential, lower Tafel slope and good durability.

Keywords: heterogeneous catalysts; metal phosphides; wrinkled structure; two dimensional; hydrogen evolution reaction

*Kai Wang[&], Bolong Huang[&], Fei Lin, Fan Lv, Minchuan Luo, Peng Zhou, Qiao Liu, Weiyu Zhang, Chao Yang, Yonghua Tang, Yong Yang, Wei Wang, Hao Wang and Shaojun Guo**

Wrinkled Rh_2P Nanosheets as Superior pH-universal Electrocatalysts for Hydrogen Evolution Catalysis

TOC figure